LETTERS

Size and albedo of Kuiper belt object 55636 from a stellar occultation

J. L. Elliot[1,2,3], M. J. Person[1], C. A. Zuluaga[1], A. S. Bosh[1], E. R. Adams[1], T. C. Brothers[1], A. A. S. Gulbis[1,4], S. E. Levine[1,5,6], M. Lockhart[1], A. M. Zangari[1], B. A. Babcock[7], K. DuPré[8], J. M. Pasachoff[8], S. P. Souza[8], W. Rosing[9], N. Secrest[10], L. Bright[3], E. W. Dunham[3], S. S. Sheppard[11], M. Kakkala[12], T. Tilleman[5], B. Berger[13], J. W. Briggs[13,14], G. Jacobson[13], P. Valleli[13], B. Volz[13], S. Rapoport[15], R. Hart[16], M. Brucker[17], R. Michel[18], A. Mattingly[19], L. Zambrano-Marin[20], A. W. Meyer[21], J. Wolf[22], E. V. Ryan[23], W. H. Ryan[23], K. Morzinski[24], B. Grigsby[24], J. Brimacombe[25], D. Ragozzine[26], H. G. Montano[27] & A. Gilmore[28]

The Kuiper belt is a collection of small bodies (Kuiper belt objects, KBOs) that lie beyond the orbit of Neptune and which are believed to have formed contemporaneously with the planets. Their small size and great distance make them difficult to study. KBO 55636 (2002 TX_{300}) is a member of the water-ice-rich Haumea KBO collisional family[1]. The Haumea family are among the most highly reflective objects in the Solar System. Dynamical calculations indicate that the collision that created KBO 55636 occurred at least 1 Gyr ago[2,3]. Here we report observations of a multi-chord stellar occultation by KBO 55636, which occurred on 9 October 2009 UT. We find that it has a mean radius of 143 ± 5 km (assuming a circular solution). Allowing for possible elliptical shapes, we find a geometric albedo of $0.88^{+0.15}_{-0.06}$ in the V photometric band, which establishes that KBO 55636 is smaller than previously thought and that, like its parent body, it is highly reflective. The dynamical age implies either that KBO 55636 has an active resurfacing mechanism, or that fresh water-ice in the outer Solar System can persist for gigayear timescales.

Multi-station observations of stellar occultations by the largest KBOs allow us to accurately measure their radii; also, we can probe for atmospheres and for small, nearby companions[4,5]. Unfortunately, the current state of the art for occultation shadow path predictions has errors greater than the radii of even the largest KBOs. Our group has been monitoring the largest and brightest KBOs for several years with telescopes at Lowell Observatory and the United States Naval Observatory, and with the Cerro Tololo Inter-American Observatory Small and Medium Aperture Research Telescope System (CTIO SMARTS), in order to reduce the astrometric errors in their orbits. We are now able to predict the location of the visibility zone on the Earth with an error of a few hundred kilometres for some KBO occultations. Still, to have a high probability of success for any given event, one must arrange for a network of observing stations that span a large part of the Earth. We set up such a network of 21 telescopes at 18 stations, spanning a distance of 5,920 km, which straddle the predicted[6] shadow path for the 2009 October 9 UT stellar occultation by KBO 55636. Details for all observing stations are given in Supplementary Table 2 and are shown on the map in Supplementary Fig. 1. Of these stations, seven could not observe owing to weather, nine reported non-detections, and two observed an occultation, both in Hawai'i: the 2.0-m Faulkes North telescope at Haleakala and a 0.36-m portable telescope at the Visitor Information Station at the Onizuka Center for International Astronomy on Mauna Kea (located at the Mauna Kea Mid Level). The light curves for the two successful stations and, for comparison, the non-detection from Leeward Community College, are shown in Fig. 1. The geocentric velocity of the shadow of KBO 55636 shadow across the Earth was 25.3 km s^{-1}, and the solar phase angle of KBO 55636 was 0.56°.

As diffraction effects[7] were unimportant in the Mauna Kea Mid-Level light curve (owing to the broad wavelength band, low time resolution and insufficient signal-to-noise ratio), we modelled the light curve as a square-well occultation that had four parameters: zero level, full-scale level, occultation mid-time and occultation duration. We also modelled the Haleakala light curve as a square well (see Supplementary Information section 4A and Supplementary Table 3 for a discussion of the parameters of a complete diffraction model). The results from the square-well model fits are given in Table 1. Approximating as a circle the geometric figure of KBO 55636 in the plane probed by the occultation, we find a radius of 143 km. The dominant factor in the error bar for the radius is the formal error in the occultation duration at the Mauna Kea Mid-Level station (11.03 ± 0.43 s; Table 1). We obtained the error in the radius from the error in the occultation duration of this station as follows. We considered three possibilities: (1) the occultation had the nominal duration fitted by the model, (2) the occultation had a shorter duration

[1]Department of Earth, Atmospheric, and Planetary Sciences, Massachusetts Institute of Technology, Cambridge, Massachusetts 02139, USA. [2]Department of Physics, Massachusetts Institute of Technology, Cambridge, Massachusetts 02139, USA. [3]Lowell Observatory, Flagstaff, Arizona 86001, USA. [4]Southern Africa Large Telescope and South African Astronomical Observatory, PO Box 9, 8935, Cape Town, South Africa. [5]United States Naval Observatory (USNO), Flagstaff, Arizona 86001, USA. [6]American Association of Variable Star Observers, Cambridge, Massachusetts 02138, USA. [7]Physics Department, Williams College, Williamstown, Massachusetts 01267, USA. [8]Astronomy Department, Williams College, Williamstown, Massachusetts 01267, USA. [9]Las Cumbres Observatory Global Telescope Network, Santa Barbara, California 93117, USA. [10]University of Hawai'i, Hilo, Hawai'i 96720-4091, USA. [11]Department of Terrestrial Magnetism, Carnegie Institution of Washington, Washington DC 20015, USA. [12]Department of Geology, University of Hawai'i, Leeward Community College, Pearl City, Hawai'i 96782, USA. [13]Amateur Telescope Makers of Boston, Westford, Massachusetts 01886, USA. [14]Dexter-Southfield Schools, Brookline, Massachusetts 02145, USA. [15]Research School of Astronomy and Astrophysics, Mt Stromlo Observatory, Weston Creek, Australian Capital Territory 2611, Australia. [16]Mt Kent Observatory, University of Southern Queensland, Toowoomba, Queensland 4350, Australia. [17]Department of Physics & Astronomy, University of Nebraska-Lincoln, Lincoln, Nebraska 68588, USA. [18]Instituto de Astronomía, Universidad Nacional Autónoma de México, Apartado Postal 877, 22800 Ensenada, Baja California, Mexico. [19]IBM, St Leonards, New South Wales 2065, Australia. [20]Nompuewenu Observatory, University of Texas Brownsville/Texas Southmost College, Brownsville, Texas 78520, USA. [21]SOFIA, Universities Space Research Association, NASA Ames, Moffett Field, California 94035, USA. [22]SOFIA, Deutsches SOFIA Institute, NASA Ames, Moffett Field, California 94035, USA. [23]Magdalena Ridge Observatory, New Mexico Tech, Socorro, New Mexico 87801, USA. [24]Department of Astronomy and Astrophysics, University of California, Santa Cruz, California 95064, USA. [25]James Cook University, Cairns, Queensland 4870, Australia. [26]Harvard-Smithsonian Center for Astrophysics, Cambridge, Massachusetts 02138, USA. [27]Observatorio Astronómico, Universidad Nacional Autónoma de Nicaragua, Managua, Nicaragua. [28]Mt John University Observatory, Lake Tekapo 7945, New Zealand.

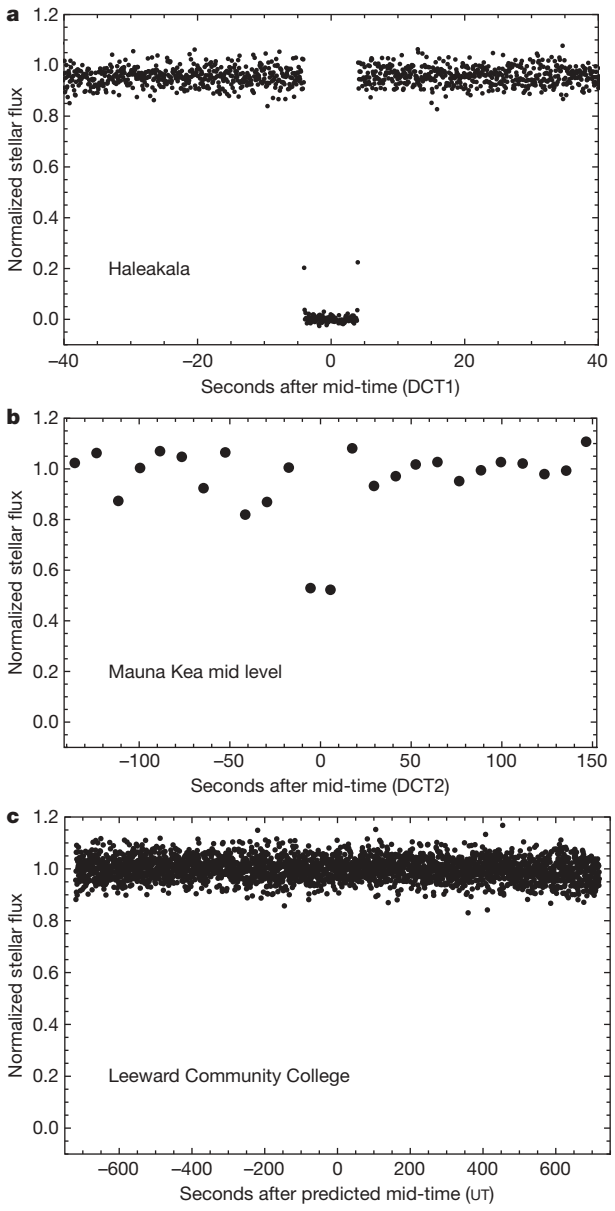

Figure 1 | Light curves for KBO 55636. a, The light curve from the Faulkes North 2.0-m telescope at Haleakala, Maui, plotted relative to the mid-time of the event according to the data-computer time at Haleakala (DCT1). An Andor Luca-R camera recorded a series of CCD frames of the field surrounding the occulted star. The sub-frame field was 90 × 90 arcsec (250 × 251 pixels), and no filter was used. Data recording started at 10:23:35.000 (DCT1) and lasted for 17.15 min. The light curve was constructed by computing the ratio of the observed flux from the occultation star to the total signal from three stars in the field. The unfiltered observations had an effective wavelength of ~700 nm. **b**, The light curve from a 0.36-m portable telescope at the Mauna Kea Mid Level, plotted relative to the mid-time of the event according to the data-computer time of the Mauna Kea Mid Level (DCT2). An SBIG ST-2000XM camera (field size: 14 × 10.5 arcmin; 1,600 × 1,200 pixels) was used with an Astrodon Luminance near-infrared-blocking filter[30] that cuts off wavelengths longer than 700 nm. Data recording started at 10:27:29 (DCT2) and lasted for 13.5 min. The light curve was constructed by computing the ratio of the observed flux from the occultation star to the total signal from five stars in the field. **c**, The light curve from the Leeward Community College 0.50-m telescope and a POETS camera (unfiltered). The field of view was 7 × 7 arcmin. The recording started at 10:17:40 UT (12 min before the predicted mid-time[6]) and lasted 24 min. The light curve was constructed by computing the ratio of the observed flux from the occultation star to the total signal from eight stars in the field. No occultation event is seen in the data. More details of the data recording at these and other stations are contained in Table 1 and Supplementary Table 2.

by one formal error of the model fit, and (3) the occultation had a longer duration by one formal error of the model fit.

These three circular solutions are presented as the entries in Supplementary Table 4, and details of the method are discussed in Supplementary Information section 4A. The nominal value of the radius is 143 km, with a range of 139–148 km between the short- and long-chord solutions. Hence, our radius determination for the circular solution is 143 ± 5 km (Fig. 2). Before our measurement, the best information about the radius of KBO 55636 for a circular sky-plane figure was an upper limit[8] of 210 km. Using the absolute magnitudes (H_V; ref. 9) supplied by W. M. Grundy (personal communication), we establish a geometric albedo of 0.88 ± 0.06 for the circular solution.

A circular approximation for the shape of KBO 55636 is not unreasonable, despite its small radius and only two occultation chords, because its rotational light curve has a peak-to-peak amplitude of only 0.08 ± 0.02 mag in the R band, with a period of about 8 hours (ref. 10). To estimate the effects on an elliptical figure, not knowing the phase of the light curve at the time of the occultation or the aspect of the rotation axis relative to the sky plane, we considered a set of ellipses with different orientations that would fit the two observed occultation chords. This analysis is discussed in Supplementary Information section 5B. Considering these elliptical possibilities increases our upper error bar on the geometric albedo to +0.15, and we find a value for the geometric albedo of $0.88^{+0.15}_{-0.06}$.

Except for the dwarf planet Eris (geometric albedo of 0.86 ± 0.07), which is likely to have an atmosphere that recoats its surface with freshly condensed ice[4], KBO 55636 has the highest geometric albedo known for a KBO[11,12]. The high albedo of KBO 55636 is probably due to a water-ice surface, as strong water-ice absorption bands have been detected in its near-infrared spectrum[1,13,14]. Haumea family members[2,3] were identified by their strong water-ice absorption bands and their similar orbital elements[1,2]. The brightest (and largest) member of this family is Haumea, and a listing of the family members is given in Table 2, along with the strengths of their water-ice bands[1]. We note that, except for Haumea and now KBO 55636, all radii

Table 1 | Light-curve model fits

Site	Telescope aperture (m)	Integration time (s)	Readout time (s)	Zero level*†	Full scale*†	Mid-time†‡	Duration (s)†	r.m.s. error*	Signal-to-noise ratio§
Haleakala	2.0	0.06861	0.00502	0.0071 ± 0.0005	0.16523 ± 0.00005	15.964 ± 0.002	8.009 ± 0.004	0.0058	108.8
MK Mid Level	0.34	5.0	7.0	0.00‖	0.0419 ± 0.0003	47.02 ± 0.21	11.03 ± 0.43	0.0025	7.5
Leeward CC	0.50	0.498	0.002	0.00‖	0.08554 ± 0.00007	NA¶	NA¶	0.0036	33.2

CC, Community College; NA, not available.
* Units are the ratio of the occulted star's flux (plus the negligible flux from the KBO) to that of the comparison stars. The r.m.s. error (1 s.d.) refers to that for a single integration.
† Error bars on all fitted parameters are 1 s.d. formal errors from the least-squares fits.
‡ Seconds after 10:29:00 UT on 2009 October 9, according to the data-computer time (DCT1, DCT2) at each station. Error bars do not include systematic offsets in the two computer clocks (see Fig. 2 legend). Note that owing to the much shorter exposure times and larger telescope used at Haleakala, the fitted occultation times for Haleakala are much more precise than those for the Mauna Kea Mid Level data.
§ The calculated ratio of the unocculted stellar flux to the r.m.s. noise for a hypothetical one second integration.
‖ Fixed parameter.
¶ No occultation was observed at Leeward Community College.

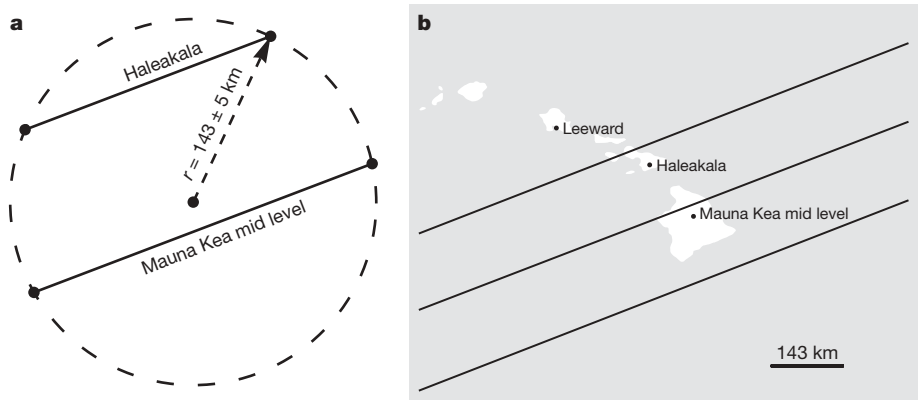

Figure 2 | Occultation chords and the radius of KBO 55636. a, The two solid lines represent the two observed occultation chords, plotted in the shadow plane and centred on KBO 55636. Alignment of the chords requires that 32.95 s be subtracted from the data-computer time (DCT2) at the Mauna Kea Mid Level, but whether we would subtract the time shift from DCT2 or add it to DCT1 does not affect the results of the analysis. The arrow illustrates the derived radius for KBO 55636 of 143 ± 5 km under the assumption of a circular figure in the sky plane (see text and Supplementary Information section 5B for a discussion of elliptical figures). The ±5 km error (1 s.d.) in the radius arises solely from the errors in the model fit for the duration of the Mauna Kea Mid Level light curve (Table 1) and corresponds to the size of the points plotted at the ends of the chords. **b**, The three solid lines represent the southern edge, centre line and northern edge of KBO 55636's occultation shadow, assuming a circular body. The positions of our observing stations at Leeward Community College, Haleakala, and the Mauna Kea (MK) Mid Level are indicated. Although the sky was clear and data were recorded, no occultation was seen at Leeward Community College.

known at present are upper limits. The final column of Table 2 gives the radius of each body under the assumption that it has the same geometric albedo as KBO 55636.

Surfaces of bodies in the outer Solar System become darkened by accumulating dust and by the removal of hydrogen[15] through the absorption of high-energy electro-magnetic and particle radiation (although the latter process applies more to carbon-based compounds). Competing with these, processes that brighten the surfaces are the condensation of fresh ice from atmospheric gases (such as nitrogen and methane on Pluto and Triton[4]), global resurfacing due to impacts[15,16], and cryovolcanism (if internal heat is available), such as observed on Saturn's high-albedo[17] satellite Enceladus[18]. Our result exacerbates the need to reconcile the bright surfaces of the Haumea collisional family (which imply a surface age of 0.1 Gyr)[19] and their apparent formation by an ancient collision (estimated to have occurred 1 Gyr ago)[2,3].

Assuming that KBO 55636 is pure water-ice, with no porosity (density = 933 kg m^{-3})[20], its mass would be 1.1×10^{19} kg (about 1.6×10^{-4} of the lunar mass). Using the definition of ref. 21 and a beaming parameter and emissivity typical of the icy satellites in the outer Solar System[21], we find that KBO 55636 has a sub-solar temperature of 49 K (which is an upper limit on the disk-averaged temperature).

A prime objective of our KBO occultation program is to detect atmospheres on KBOs, and the likely candidates for atmospheres are those objects showing bands of N_2 and CH_4 ices in their spectra, such as Eris, Sedna and Makemake[22]. KBO 55636 would not be expected to hold an atmosphere of light gases owing to its very small mass, but using the light-curve modelling methods that we employed for Charon[23,24], we can give a 3 s.d. formal limit of $\sim 2 \times 10^{15}$ cm^{-3} for the surface number density of a heavy gas, such as Xe (for an isothermal atmosphere at a temperature of 49 K).

Another objective of our occultation program is to search for previously unknown companions. Although the space sampled was sparse, no evidence of any companion was noted in any of the data sets obtained.

Received 2 February; accepted 16 April 2010.

1. Brown, M. E., Barkume, K. M., Ragozzine, D. & Schaller, E. L. A collisional family of icy objects in the Kuiper belt. *Nature* **446,** 294–296 (2007).
2. Ragozzine, D. & Brown, M. E. Candidate members and age estimate of the family of Kuiper belt object 2003 EL61. *Astron. J.* **134,** 2160–2167 (2007).
3. Schlichting, H. E. & Sari, R. The creation of Haumea's collisional family. *Astrophys. J.* **700,** 1242–1246 (2009).
4. Elliot, J. L. & Kern, S. D. Pluto's atmosphere and a targeted-occultation search for other bound KBO atmospheres. *Earth Moon Planets* **92,** 375–393 (2003).
5. Reitsema, H. J., Hubbard, W. B., Lebofsky, L. A. & Tholen, D. J. Occultation by a possible third satellite of Neptune. *Science* **215,** 289–291 (1982).
6. Zuluaga, C. A., Bosh, A. S., Person, M. J. & Elliot, J. L. 55636.20091009 Occultation October 09, 2009. ⟨http://occult.mit.edu/research/occultations/kbo/55636/55636.20091009/index.html⟩ (2009).

Table 2 | Radii and albedos of Haumea-collisional-family members

KBO number	Name (designation)	Strength of water absorption band[1] (%)	Radius (km)	Geometric albedo, p_V	Radius for $p_V = 0.88$ (km)
136108	Haumea (2003 EL_{61})	55 ± 1	1,000 × 750 × 500 (refs 22, 25)	~0.73 (refs 22, 25)	~600*
55636	**(2002 TX_{300})**	**65 ± 4**	**143 ± 5**†	**$0.88^{+0.15}_{-0.06}$**‡	**143 ± 5**†
	Haumea I[26]	87 ± 11	<250§ (ref. 27)	>0.65	~130
	(2005 RR_{43})	60 ± 7			~109
120178	(2003 OP_{32})	77 ± 4			~108
24835	(1995 SM_{55})	43 ± 13	<352 (ref. 11)	>0.053 (ref. 8)	~87
19308	(1996 TO_{66})	65 ± 5	<451 (ref. 11)	>0.027 (ref. 8)	~80
	Haumea II	IR colours of water ice[28]	<120§ (ref. 27)	>0.65	~ 70
	(2003 UZ_{117})	Strong[6]			~66
86047	(1999 OY_3)	IR colours of water ice[2]			~35
	(2003 SQ_{317})	IR colours of water ice[14]			
	(2005 CB_{79})	Strong[29]			

Data taken from refs 1 and 2 unless otherwise specified. Haumea I (also known as Hi'iaka) and Haumea II (also known as Namaka) are respectively the brightest and second brightest satellites of Haumea. IR, infrared. Bold font shows data for KBO 55636.
* Geometric effective radius.
† For a circular solution (see text). The error bar is 1 s.d. error from the fitted solution.
‡ The error bars are 1 s.d. errors with the asymmetry accounting for possible elliptical solutions (see text).
§ For $p_V > 0.65$.

7. Nather, R. E. & Evans, D. S. Photoelectric measurement of lunar occultations. I. The process. *Astron. J.* **75,** 575–582 (1970).
8. Brucker, M. J. *et al.* High albedos of low inclination classical Kuiper belt objects. *Icarus* **201,** 284–294 (2009).
9. Bowell, E. *et al.* in *Asteroids II* (eds Binzel, R. P., Gehrels, T. & Matthews, M. S.) 524–556 (Univ. Arizona Press, 1989).
10. Sheppard, S. S. & Jewitt, D. Hawaii Kuiper belt variability project: an update. *Earth Moon Planets* **92,** 207–219 (2003).
11. Grundy, W., Noll, K. & Stephens, D. Diverse albedos of small trans-neptunian objects. *Icarus* **176,** 184–191 (2005).
12. Stansberry, J. A. *et al.* in *The Solar System beyond Neptune* (eds Barucci, M. A., Boehnhardt, H., Cruikshank, D. P. & Morbidelli, A.) 161–179 (Univ. Arizona Press, 2008).
13. Licandro, J. *et al.* The methane ice rich surface of large TNO 2005 FY9: a Pluto-twin in the trans-neptunian belt? *Astron. Astrophys.* **445,** L35–L38 (2006).
14. Snodgrass, C., Carry, B., Dumas, C. & Hainaut, O. Characteristics of candidate members of (136108) Haumea's family. *Astron. Astrophys.* **511,** 1–9 (2010).
15. Gil-Hutton, R. Color diversity among Kuiper belt objects: the collisional resurfacing model revisited. *Planet. Space Sci.* **50,** 57–62 (2002).
16. Luu, J. & Jewitt, D. Color diversity among the Centaurs and Kuiper Belt objects. *Astron. J.* **112,** 2310–2318 (1996).
17. Verbiscer, A. J., French, R. G. & McGhee, C. A. The opposition surge of Enceladus: HST observations 338–1022 nm. *Icarus* **173,** 66–83 (2005).
18. Spencer, J. R. *et al.* in *Saturn from Cassini-Huygens* (eds Dougherty, M., Esposito, L. W. & Krimigis, S.) 683–724 (Springer, 2009).
19. Rabinowitz, D. L., Schaefer, B. E., Schaefer, M. & Tourtellotte, S. W. The youthful appearance of the 2003 EL_{61} collisional family. *Astron. J.* **136,** 1502–1509 (2008).
20. Hobbs, P. V. *Ice Physics* 1st edn 348 (Oxford Univ. Press, 1974).
21. Spencer, J. R., Lebofsky, L. A. & Sykes, M. V. Systematic biases in radiometric diameter determinations. *Icarus* **78,** 337–354 (1989).
22. Brown, M. E. in *The Solar System beyond Neptune* (eds Barucci, M. A., Boehnhardt, H., Cruikshank, D. P. & Morbidelli, A.) 335–344 (Univ. Arizona Press, 2008).
23. Gulbis, A. A. S. *et al.* Charon's radius and atmospheric constraints from observations of a stellar occultation. *Nature* **439,** 48–51 (2006).
24. French, R. G. & Gierasch, P. J. Diffraction calculation of occultation light curves in the presence of an isothermal atmosphere. *Astron. J.* **81,** 445–451 (1976).
25. Rabinowitz, D. L. *et al.* Photometric observations constraining the size, shape, and albedo of 2003 EL61, a rapidly rotating, Pluto-sized object in the Kuiper Belt. *Astrophys. J.* **639,** 1238–1251 (2006).
26. Brown, M. E. *et al.* Satellites of the largest Kuiper belt objects. *Astrophys. J.* **639,** L43–L46 (2006).
27. Ragozzine, D. & Brown, M. E. Orbits and masses of the satellites of the dwarf planet Haumea (2003 EL61). *Astron. J.* **137,** 4766–4776 (2009).
28. Fraser, W. C. & Brown, M. E. NICMOS photometry of the unusual dwarf planet Haumea and its satellites. *Astrophys. J.* **695,** L1–L3 (2009).
29. Schaller, E. L. & Brown, M. E. Detection of additional members of the 2003 EL61 collisional family via near-infrared spectroscopy. *Astrophys. J.* **684,** L107–L109 (2008).
30. Astrodon:. Astrodon astronomy filters. ⟨http://www.astrodon.com/products/filters/⟩ (2008).

Supplementary Information is linked to the online version of the paper at www.nature.com/nature.

Acknowledgements We are grateful to W. M. Grundy for supplying H_V magnitudes from his database and for discussions of water-ice surfaces in the outer Solar System; to W. B. McKinnon for discussions of the physical state of water-ice at low temperatures; to E. D. Schmidt for use of the telescope and participating in the observations at Behlen Observatory; to B. Carter for help in obtaining telescope time at Mt Kent, and to L. A. Young for assisting with the McDonald observations. We thank D. Byrne of the Visitor Information Station at the Onizuka Center for International Astronomy on Mauna Kea for use of their equipment and facilitating the observations from their site. J.W. thanks E. Gates of Lick Observatory, and E. Becklin, E. Pfueller, M. Wiedemann and M. Burgdorf of SOFIA, for support of his observations. B. Sicardy provided several comments that improved the paper. Occultation research at MIT and Williams College is supported by NASA and NSF.

Author Contributions J.L.E. helped plan the observations, consulted on the occultation prediction, analysed the data, and wrote the paper. M.J.P. organized the observers, performed observations from Brownsville, Texas, and consulted on the prediction, data reduction, text and figures. C.A.Z. analysed the data for the stellar occultation prediction and constructed the light curves. A.S.B. directed the data analysis for the occultation prediction. E.R.A. wrote the light-curve generation software. S.E.L. made astrometric observations and performed observations of the occultation from the USNO in Flagstaff. M.L. designed and built 12 PICO camera systems and attempted observations from Cairns. J.M.P. arranged for observations at several sites and helped to plan the observations. S.P.S. consulted on the design of the PICO. L.B., E.W.D., S.S.S. and T.T. supplied astrometric data for the occultation prediction. D.R. provided information used to derive the geometric albedo of KBO 55636. Authors identified in Supplementary Table 2 were responsible for the observations. All authors were given the opportunity to review the results and comment on the manuscript.

Author Information Reprints and permissions information is available at www.nature.com/reprints. The authors declare no competing financial interests. Readers are welcome to comment on the online version of this article at www.nature.com/nature Correspondence and requests for materials should be addressed to J.L.E. (jle@mit.edu).